Design of Seismic Isolated Bridge in Soft Ground

D. W. Chang, P. H. Huang, H. C. Chen, S. Liu, T. Y. Tang & C. K. Su
CECI Engineering Consultants, Inc., Taiwan

SUMMARY:

The protective system, installed between the superstructure and substructure, is a kind of seismic isolation bearing that increases the structural damping and horizontal flexibility of bridges. By using the inelastic mechanism of bearing, the essential period of structure is extended and the lateral force of piers are dispersed and lessened. That made it capable of providing economical and safe designs. On the other hand, the debatable properties of soft ground include a full and partial settlement, negative skin friction in pile foundations, consolidation settlements from loadings, bearing capacity of foundations, soil liquefaction and large variability of structural behaviors during earthquakes. Compared with hard site, the period between short and moderate-to-long period ranges of the site-dependent normalized design response spectrum in soft site stipulated by seismic design code for bridges is longer. This amplifies the resonance seismic excitation response and puts the isolation system at risk. Furthermore, the designed seismic lateral force for bridges can not be reduced within the adequate displacements by increasing the period. Thus, the purpose of this study is to discuss the applicability of isolation system in soft ground and investigate the notable issues in practical bridge design stages.

Keywords: isolation system, soft ground, seismic excitation

1. INTRODUCTION

Based on the purposes of reducing construction timeline, decreasing environmental impact, improving construction safety, reducing life-cycle costs, and accelerating trade harbor development, which were comprising the vantage points of adopting precast concrete girders and piers (Ou et al. 2007), the connecting viaduct for Kaohsiung Harbor project in Taiwan was then constructed with prefabricated super and substructure construction in recent years. In this seismic design philosophy of structures, to extensively use these types of element in regions of low and high seismicity as well, the isolation system of distinct bearings were hence employed cooperatively with prefabricated ones in the design of bridge (Huang et al. 2010). Due to concepts of both box-girder and segmental column were designed to remain within the elastic range in the isolated bridge, the behaviors of those elements aren't discussed herein to enhance neither hysteretic energy dissipation nor the seismic responses. The interest is merely concentrated on the dynamic characteristics and earthquake excitations of bridge in soft site with the LRB isolation system revealing a bilinear hysteretic property based on an analytical 3D SAP2000 (2010) bridge model.

In this study, the static design process is drawn up according to the practical application of LRB technologies with interpreting the simulated method of isolated system (AASHTO 2010). After describing the details of targeted viaduct and geology in Kaohsiung Harbor, the site-adjusted design

response spectrum is then illustrated in contrast to the seismic excitations investigating from free-field strong motions surrounded the site. Furthermore, to test the feasibility of proposed model, the static, response spectrum, and nonlinear time history analyses of the isolated bridge are particularly carried out utilizing the behaviors of pier shear force with different boundary conditions and analysis methods. As practical isolated bridge design plan, the evaluation processes and devisable results presented in this paper are expected to provide useful perception on the soil-structure interaction (SSI) and site-specific excitation (SSE) effects in earthquake engineering (Tongaonkar and Jangid 2003, Dicleli et al. 2005).

2. PRACTICAL DESIGN PROCEDURE FOR SEICMIC ISOLATED BRIDGE

According to seismic design specifications of bridges (2008) published by Ministry of Transportation and Communications in Taiwan, the design procedure for seismic isolated bridge can be expressed as flowchart shown in Fig. 2.1 and the following statement of static design procedure for LRB can be addressed step by step as follows:

(1) Assume the design displacement at the center of gravity of the superstructure, D_s.

(2) The horizontal displacement of substructure (D_p) is estimated as

$$D_P = \frac{F_d}{K_P} = \frac{Q_d + K_d D_s}{K_P + K_d} \tag{1}$$

where F_d is the shear force in the isolator unit at displacement D_d, Q_d is the characteristic strength of the isolator unit, K_d is the post-yielding stiffness of the bilinear hysteresis curve, K_P is stiffness of the substructure protected by the isolation unit.

(3) Use D_s and D_p from steps 1 and 2 to obtain the displacement of isolator unit:

$$D_d = D_s - D_P \tag{2}$$

(4) Apply D_d from step 3 to determine the effective stiffness of isolator:

$$K_{eff} = \frac{Q_d + D_d \cdot K_d}{D_d} \tag{3}$$

(5) The equivalent viscous damping ratio (ξ_{eq}) of the isolation system shall be calculated as:

$$\xi_{eq} = \frac{E_D}{2\pi E_s} = \frac{E_D}{2\pi K_{eff} D_d^2} = \frac{4Q_d(D_d - D_y)}{2\pi K_{eff} D_d^2} \tag{4}$$

where D_y is yield displacement of isolator, E_D is the energy dissipation capacity (EDC) area which shall be taken as the sum of the areas of the hysteresis loops of all isolator units.

(6) In calculating the effective stiffness, the configuration, flexibility, and individual stiffness of the isolator units and substructure shall be taken into account.

$$K_{e,i} = \frac{K_{eff,i} K_{p,i}}{K_{eff,i} + K_{p,i}} \tag{5}$$

where $K_{p,i}$ is the elastic stiffness of i-th pier, $K_{eff,i}$ is the sum of the effective linear springs of all bearings above i-th pier.

(7) The effective period T_e of bridge can be expressed as

$$T_e = 2\pi \sqrt{\frac{W}{g \sum K_{e,i}}} \tag{6}$$

(8) The effective damping ratio is rationally defined in the form of

$$\xi_e = \frac{\sum K_{eff,i} D_{d,i}^2 \left[\xi_{eq,i} + \xi_{p,i} \dfrac{K_{eff,i}}{K_{p,i}} + \xi_{T,i} \dfrac{K_{eff,i}}{K_{T,i}} + \xi_{R,i} \dfrac{K_{eff,i} H^2}{K_{R,i}} \right]}{\sum K_{eff,i} D_{d,i}^2 \left[1 + \dfrac{K_{eff,i}}{K_{p,i}} + \dfrac{K_{eff,i}}{K_{T,i}} + \dfrac{K_{eff,i} H^2}{K_{R,i}} \right]} \tag{7}$$

where the component damping ratios $\xi_{eq,i}$, $\xi_{p,i}$, $\xi_{T,i}$ and $\xi_{R,i}$ of i-th pier represent the equivalent viscous damping ratio of the isolation system, the inherent damping ratio of the substructure, the viscous damping ratios of foundation corresponding to the elastic lateral stiffness $K_{T,i}$ and rotational stiffness $K_{R,i}$, respectively; H is the height from top of foundation to the center of gravity of the superstructure (Hwang et al. 1996).

(9) The design spectral response acceleration (S_{aD}) for general sites, adjusted using the correction coefficients B_1 provided in Tab. 2.1, shall be determined in accordance with Equation (8):

$$S_{aD} = \frac{S_{D1}}{B_1 T_e} \tag{8}$$

where S_{D1} denote the site adjusted spectral response acceleration at 1 second in Taiwan, which had modified by site coefficients to include local site effects (Loh et al. 2001).
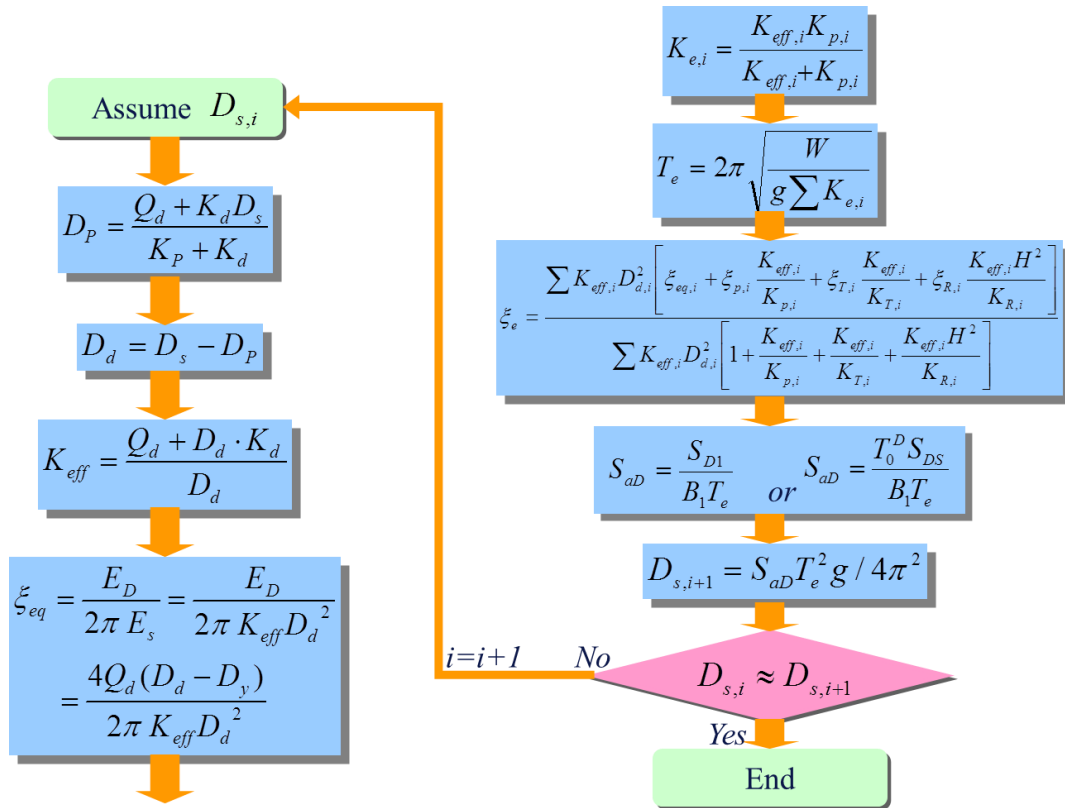
Table 2.1. Damping correction coefficients B_S and B_1

Damping (percentage of critical)	B_S	B_1
<2	0.80	0.80
5	1.00	1.00
10	1.33	1.25
20	1.60	1.50

(10) The design lateral displacement D_s can be finally expressed as

$$D_s = S_{aD} T_e^2 g / 4\pi^2 \tag{9}$$

(11) Confirming the convergent of the corresponding sequence converges for D_s between step 10 and 1 until obtaining a desired result.

Figure 2.1. Flowchart of the design procedure for seismic isolated bridge

3.   BRIDGE PROPERTIES

As shown in Fig. 3.1, the total length of the targeted bridge is 207 m and the width of box-girder is 11 m. The bridge deck is continuous from pier 1 to pier 6 and is supported by seismic isolation bearing over the top of single-type piers. All piers have identical geometry but heights (H) varying between 8.53 and 8.88 m. The longitudinal and transverse stiffness are hence differing from 46,227 to 50,714 and 52,750 to 59,513 tf/m, respectively. The total weight of superstructure is approximately 5,247 tf without adjoining unit loading. Two LRBs and one shear steel box are placed at each substructure location. The shear steel box is used as internal displacement limiting device.
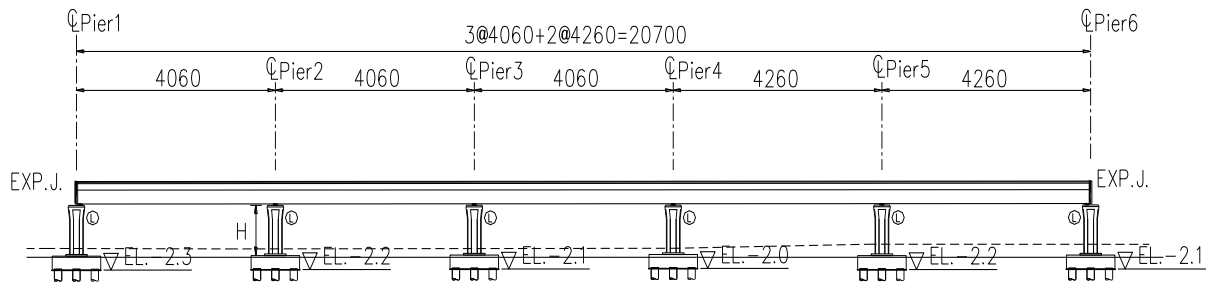
(a) Longitudinal elevation of the bridge
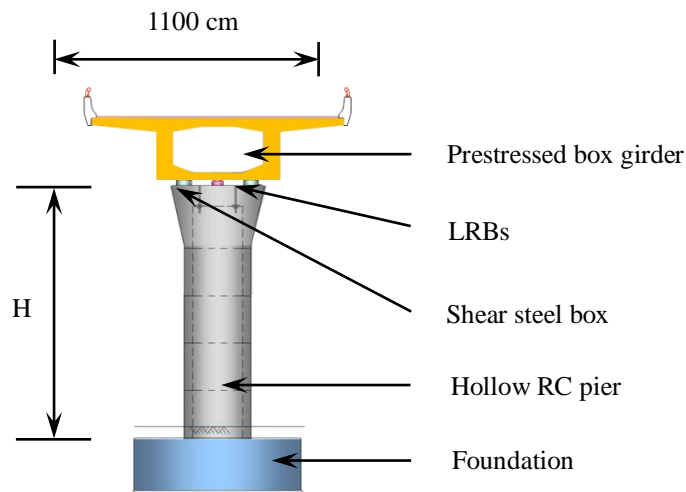
(b) Transverse section of the bridge

Figure 3.1. Geometric details of bridge (all dimensions are in cm)


4. GEOTECHNICAL PROPERTIES IN SITE

The sited area of connecting viaduct belonged to the alluvial plain with flat topography. As shown in Fig. 4.1, the foundations lay in Holocene sediments consisting of alternating layers of cohensionless sand and clay, mostly soft to stiff, and loosely laid loose rocks. The water table was close to the natural ground surface while the correlated standard penetration test N values (SPT-N) were all less than or equal to five. The density of silty sand strata was in loose to medium condition for the first 30 m and the SPT-N values were in the range of 5 to 35. The layer of next 30 m was mainly composed of clay strata with SPT-N=10~50 while the deeper layer was consisting of sand. Combined all-casing piles and plate foundations with piles over 30~50 m long were usually be used in this area.

Figure 4.1. Regional geological map of the Kaohsiung port

5. ANALYTICAL MODEL OF ISOLATED BRIDGE

The superstructure and substructure of bridge, including deck width, number of spans, type of girder, number of girders per span, main spans length, superimposed loading, cross-section of pier, heights of each column and dimension of foundation, have to be considered in seismic energy response of seismically isolated bridge. In this paper, the isolated bridge system details were been modeled as shown in Fig. 5.1 as a discrete model. In this figure, the girder and pier are simulated by elastic beam-column element while the soil spring represented the SSI effects. In addition, the isolation bearing is used for the structural system of bridge and its restoring force is simulated by a bilinear model pondered stiffness and damping respectively.
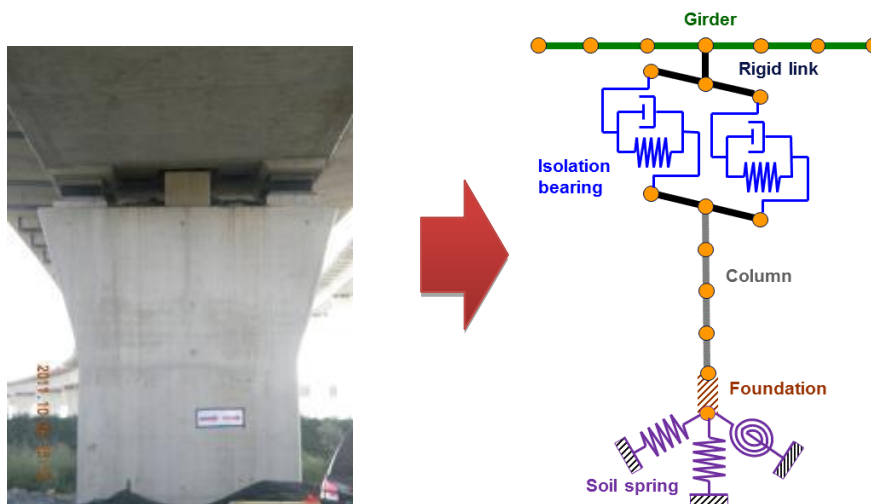

Figure 5.1. Mathematical model of isolated bridge

6. SEISMIC EXCITATIONS

Five ground motion time histories consist of actual earthquakes with magnitudes larger than 6.0 are used in this study. These motions were recorded to Central Weather Bureau (CWB) earthquake reports in Taiwan. The chosen ground motions were selected from source-to-site distances closed to Kaohsiung City and the free-field strong motion stations (i.e. KAU045, KAU087 and KAU092) were surveyed. The seismic events, stations and the assumed magnitude (M_L) associated with each ground motion are presented in Tab. 6.1. The scaling spectra calculated from those time history records are amplified their amplitudes to $0.4S_{DS}$ as shown in Fig. 6.1. Comparing the periods between short and moderate-to-long period ranges illustrated in Fig. 6.1 with design response spectrum, these recorded time histories indicated that the extents of peak acceleration region almost distributed longer than the ranges as defined in code. The analytical results shows the variability of seismic excitation responses in soft ground, which should be considered into multimode response spectrum and nonlinear time history analysis procedures as SSE effects, unequivocally.

Table 6.1. List of ground motions

Record ID	Seismic event	Magnitude(M_L)	Depth(km)	Station(observed in Kaohsiung)
1	1999/10/22 Chiayi	6.4	12.1	KAU045
2	2006/04/01 Taitung	6.2	7.2	KAU045
3	2006/04/01 Taitung	6.2	7.2	KAU087
4	2010/03/04 Jiaxian	6.4	22.6	KAU045
5	2010/03/04 Jiaxian	6.4	22.6	KAU092
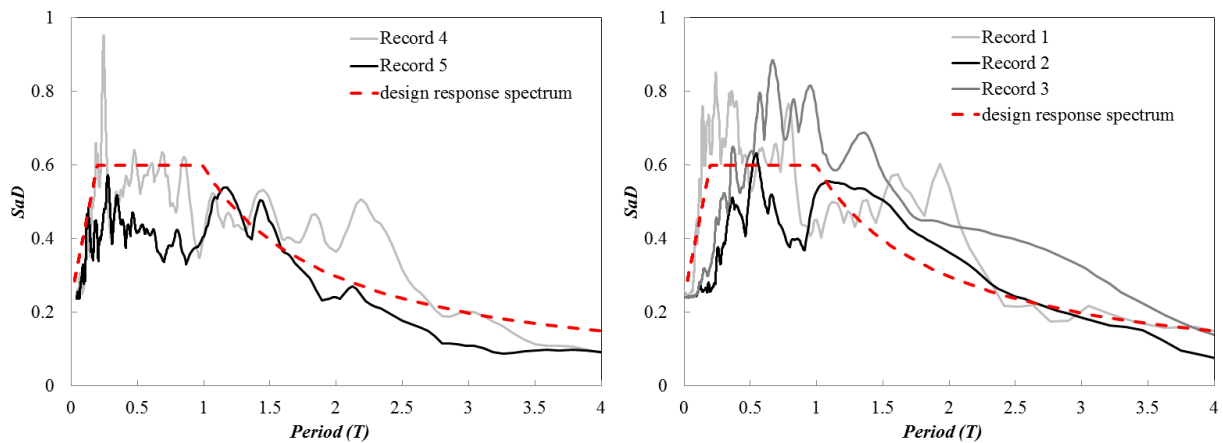
Figure 6.1. Response spectra

7. ANALYSES RESULTS AND DISCUSSION

The main design displacements of viaduct are controlled under 16 cm approximately to avoid large isolation drifts and keep both of the deck end spaces and expansion joints within maintenance limits in preliminary static design procedure shown in Fig. 2.1. The response spectrum analysis (RSA) procedures are then performed with damping ratio ξ≈18% to verify the results obtained from that procedure without SSI. After that, three synthetic ground motions, chosen from records as listed in Tab. 6.1, are scaled such that their response spectra match that of specifications' definition (2008) to accomplish nonlinear time history analyses (NTHA). Those obtained results are tabulated in Tab. 7.1. As can be seen from the table that the pier top shear force (V_P) responses are significantly executed alike in RSA and NTHA as compared with the results of static design procedure one.

Tab. 7.1. Seismic shear forces transferred to substructures in preliminary static design criteria

Substructure	V_P (tf)				
	Static design procedure	RSA	NTHA 1	NTHA 2	NTHA 3
Pier 1	151	149	147	138	145
Pier 2	299	292	289	275	285
Pier 3	299	292	292	269	287
Pier 4	299	292	292	269	287
Pier 5	299	292	289	275	285
Pier 6	151	149	143	136	142

In order to conduct further investigation into SSI and SSE effects, five site-specific ground motions as depicted in Fig. 6.1 are performed utilizing the shear forces in pier top with different boundary. Tab. 7.2 and 7.3 display V_P at each substructure location considering these five motion effects with additional viscous damping ratio provided by LRB. The obtained results, which are comparing the average V_P estimated from these versus records with that in static design procedure, have shown the extremely seismic shear forces induced by unpredictable SSI and SSE effects.

Table 7.2. Seismic shear forces in pier top considered site-specific excitations without SSI effects

Substructure	V_P (tf)					
	Record 1	Record 2	Record 3	Record 4	Record 5	**Average**
Pier 1	163	166	300	224	121	195
Pier 2	320	327	589	441	237	383
Pier 3	320	327	590	441	238	383
Pier 4	321	328	591	442	238	384
Pier 5	320	327	589	440	237	383
Pier 6	163	167	300	225	121	195

Table 7.3. Seismic shear forces in pier top considered site-specific excitations with SSI effects

Substructure	V_P (tf)					
	Record 1	Record 2	Record 3	Record 4	Record 5	**Average**
Pier 1	171	182	322	233	129	207
Pier 2	328	349	618	446	248	398
Pier 3	329	350	619	447	249	399
Pier 4	329	350	619	447	249	399
Pier 5	328	349	618	446	248	398
Pier 6	172	182	323	233	130	208

8. CONCLUDING REMARKS

Due to the associated guidelines for the design of bridges with seismic isolation system is available in the seismic design code without specified the detailed design procedure, the SSI and SSE effects, highly recommended in the relative journal papers and novel design reports in last decade (Ucak and Tsopelas 2008, Haque 2010, Chen et al. 2011), are performed into nonlinear analytical model in this study. Based on trends of observable results presented in this paper, the following conclusions and recommendations may be made:

1. Comparing the seismic excitation responses of actual earthquakes recorded in site with site-adjusted design response spectrum, it can be found that the periods among peak acceleration regions are ranged unexpectedly longer than what regulated in specifications (2008). As consequent, the design of the isolation system has to ponder particularly to evade resonance effects.

2. In the case study of preliminary design process excluding SSI effects, the obtained results of RSA and spectrum-compatible NTHA are closed to the one derived in practical design procedure. It

reveals the accuracy of suggested static procedure and analytical model.

3. For the substructure behavior represented by the seismic shear force in pier top, the results exhibit that SSE effects might be mostly detrimental to the dynamic response of the bridge pier in soft site. Accordingly, for safe design purposes, the SSE effects must be explicitly considered as the observed increases in the average pier shear were of the order of 30% for excluding SSI and even 35% for including SSI as compared with the case of practical design procedure.

4. As the results shown in this study, the benefit of the period lengthening isn't recommended in this case, and the advantage of increase of viscous damping is barely adopted.

5. In order to lessen traffic disruption, improve construction quality and reduce environmental impact, the intentions of applying segmental precast concrete piers with LRB system, which has been proved and recommended not adopting the advantage of period elongation in this project, are still reasonable and benefited from comprehensives consideration. It is conclude that the progressive analytical methods and manifold considerations presented in this study could be applicable for isolation systems in soft ground.

REFERENCES

AASHTO (2010), Guide Specifications for Seismic Isolation Design, Third Edition, American Association of State Highway and Transportation Officials, 444 North Capitol Street, NW Suite 249, Washington, DC 20001.

Chaudhary, M. T. A. (2004). Influence of Pier Stiffness Degradation on Soil-Structure Interaction in Base-Isolated Bridges, *Journal of Bridge Engineering*, *ASCE*, **Vol. 9: 3**, 287-296.

Chen, L. K., Jiang, L. H., Long, W. G. and Wang, L. P. (2011). Research on Seismic Response and Damping Effect for High-Speed Railway Seismic Isolated Bridge, *The Open Civil Engineering Journal*, **No. 5**, 163-167.

Dicleli, M., Mansour, M. Y. and Constantinou, M. C. (2005). Efficiency of Seismic Isolation for Seismic Retrofitting of Heavy Substructured Bridges, *Journal of Bridge Engineering*, **Vol 10:4**, 429-441.

Dicleli, M., Albhaisi, S. and Mansour, M. Y. (2005). Static Soil–Structure Interaction Effects in Seismic-Isolated Bridges, *Practice Periodical on Structural Design and Construction*, **Vol 10: 1**, 22-33.

Haque, M. N., Bhuiyan, A. R. and Alam, M. J. (2010). Seismic response analysis of base isolated highway bridge: Effectiveness of using laminated rubber bearings, *IABSE-JSCE Joint Conference on Advances in Bridge Engineering-II*, August 8-10, 2010, Dhaka, Bangladesh.

Hwang, J. S., Chiou, J. M. and Sheng, L. H. and Gates, J. H. (1996). A Refined Model for Base-Isolated Bridges with Bi-Linear Hysteresis Characteristics, *Earthquake Spectra, the Professional Journal of Earthquake Engineering Research Institute*, **Vol 12: 2**, 245-274.

Huang, P. H., Chen, H. C., Chen, B. H., Chi, S. R. and Su, C. K. (2010). A Study on the Seismic Isolation System of Bridge in Soft Ground, *The Tenth National Conference on Structural Engineering*, Tao-Yuan, Taiwan, 1-3 Dec., Paper No. 181(In Chinese).

Loh, C. H., Chai, J.-F., Liao, W.I and Teng, T.J. (2001). The Current Development of Seismic Design Code in Taiwan, *Proceedings of US-Japan Workshop on Performance Based Design of Reinforced Concrete Structures*, Seattle, 17-18, September.

Ou, Y. C., Chiewanichakorn, M., Aref, A. J. and Lee, G. C. (2007). Seismic Performance of Segmental Precast Unbonded Posttensioned Concrete Bridge Columns, *Journal of Structural Engineering*, **Vol 133:11**, 1636-1647.

SAP2000 (2010). CSI Analysis Reference Manual, Berkeley, California, USA.

Seismic Design Specifications of Bridges (2008). Ministry of Transportation and Communications, Taipei, Taiwan.

Ucak, A and Tsopelas, P. (2008). Effect of Soil–Structure Interaction on Seismic Isolated Bridges, *Journal of Structural Engineering*, *ASCE*, **Vol 134: 7**, 1154-1164.